Journal of Energy Storage 50 (2022) 104562

Contents lists available at ScienceDirect

Journal of Energy Storage

journal homepage: www.elsevier.com/locate/est

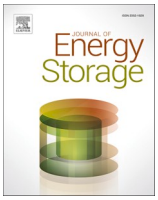

Research Papers

A rapid capacity evaluation of retired electric vehicle battery modules using partial discharge test

Mohamed Ahmeid [a,b,*], Musbahu Muhammad [c], Simon Lambert [a], Pierrot S. Attidekou [a,b], Zoran Milojevic [a,b]

[a] School of Engineering, Newcastle University, Newcastle upon Tyne NE1 7RU, UK
[b] The Faraday Institution, Quad One, Harwell Science and Innovation Campus, Didcot OX11 0RA, UK
[c] School of Computing Engineering & Digital Technologies, Teesside University, T1 3BX Middlesbrough, UK

ARTICLE INFO

Keywords:
Lithium-ion batteries
State of charge
Incremental capacity analysis
Discharge capacity
Battery modules
Retired modules
Electric vehicles

ABSTRACT

As the number of EVs hitting the roads increased, dealing with their waste such as retired LIBs become an increasingly important issue to guarantee sustainability and reduce the cost of the recycling process. This imposes establishing a practical and cost-effective gateway testing framework to sort the retired batteries based on their remaining energy capacity, and to assign them for repurposing/reusing or for recycling to extract the raw materials. Therefore, the purpose of this paper is to introduce a practical sorting method that entails the use of incremental capacity, equivalent circuit model, and manipulated coulomb counting to evaluate the full capacity of retired battery modules based on partial discharge profile. The feasibility of the proposed method is demonstrated on both truncated full discharge profile and pulse discharge profile from partially charged battery. For the investigation, 48 lithium-ion modules from retired 24 kWh Nissan Leaf battery pack are used. The experimental results show that the proposed method is capable to estimate the full capacity with a maximum error of 5%. Furthermore, a considerable reduction in the test time is achieved, with only the terminal voltage and discharge current are used, which is of great practical significance to the battery recycling industry where the cost and time are dominant.

1. Introduction

In recent years, the development of electric vehicles (EVs) has gained great momentum in the transportation industry due to the inherent advantages over internal combustion engine vehicles in terms of improved performance and zero on-highway greenhouse gas emissions [1]. Broad and rapid deployment of EVs in the world vehicle fleet is widely perceived as a critical and necessary contribution to addressing the growing concern over global warming and the issue of environmental pollution. Owing to their superior performance in both power and energy density as well as proven long lifespan, Lithium-ion batteries (LIBs), in their various guises, have for some time been the overwhelmingly dominant candidate as a power source in hybrid and EVs [2,3]. With the expanding EV market, the use of LIBs is expected to increase rapidly over the next few decades [4]. Indeed, the global market for EVs is predicted to grow up to 33% of the global car fleet by 2040 [5]. Combined with an increase in the average capacity of EV batteries implies an exponential increase in the number of LIBs entering the market and, whilst LIBs are typically longer-lived than alternatives, their finite lifetime coupled with the market growth equally implies significant and increasing numbers of batteries will ultimately reach end-of-life (EoL) in their primary application – the EV [6,7]. It is important to consider that there are several ecological, technical, economic, and social responsibility issues surrounding the sourcing and extraction of many of the constituent material components of LIBs, such as the lithium itself, cobalt, nickel and others as well as recognising that these resources are finite in nature [8–11]. As such, doctrines such as the waste hierarchy frameworks direct the battery-storage industry, and society in general, to prioritise waste prevention, reuse and recycling respectively above recovery and disposal in order to create a better circular economy around batteries and diminish social, economic and environmental harm [6]. This entails establishing safe and efficient recycling facilities to assess and process LIBs from EVs for reuse or recycling at significant quantities [12].

The concept of EoL for batteries is complex; a battery may well be considered to have deteriorated in either capacity or power performance

* Corresponding author at: School of Engineering, Newcastle University, Newcastle upon Tyne NE1 7RU, UK.
E-mail address: mohamed.ahmeid1@ncl.ac.uk (M. Ahmeid).

https://doi.org/10.1016/j.est.2022.104562
Received 10 June 2021; Received in revised form 11 February 2022; Accepted 28 March 2022

to a point beyond the acceptable capabilities for the original vehicle application. In this case it can clearly be considered to be at EoL for that application, however other applications may exist for which the performance deterioration is not a significant issue. A prime example is the comparison between the vehicle applications, where both absolute power and energy as well as the respective densities are key factors, to that of stationary storage where the density requirements are less stringent [13]. Prioritising the preclusion of recycling, recovery, and disposal in favour of prevention and reuse, coupled with the possibility of repurposing batteries which are only at EoL for EV applications leads to the concept of so called second-life batteries (recognising that ultimately the lifetime of the battery remains finite and that at some point it can no longer be reused and must be recycled) [4,14].

In this sense, there is clearly a requirement to be able to make quantifiable and reliable judgements on whether batteries which have been in primary use can be (1) reused in the primary application (2) repurposed to a secondary (or tertiary etc.) application or (3) no longer be economically deployed in any application and must be released for recycling. Indeed, developing a reliable assessment method is considered to be one of the most important steps towards understanding the conditions of the batteries and streamlining waste processing so that the priorities of the waste hierarchy are addressed. Well defined and designed testing protocols have the potential not only to give predictive performance data for non-primary usage cases but also to forecast the status of the evolution of some of the constituent materials which may be of use to downstream process design or operation. This ensures safety and reliability either during second use or within the recycling process to segregate and repurpose battery cell constituents.

To attain a vigorous and practical assessment method, battery state of health (SOH) must be accurately determined. The SOH indicates the status of degradation for the LIB that reflects its ability to deliver and store electrical energy in percentage form compared with a fresh battery [15]. For instance, in an EV battery, the SOH is usually quantified based on the decrease in capacity that is directly associated with the driving range, and deterioration in its power capability which is determined by the increase in battery resistance [16]. Therefore, the key task for the assessment method is to group the state-of-the-art methodologies used in SOoH estimation of LIBs and utilise them in gateway testing for EoL automotive batteries in an industrial environment.

In EVs, the LIBs are usually integrated in parallel or in modules to boost the capacity and driving range and the modules are grouped in series to form the packs hence to meet the high voltage demand [17]. However, existing research on battery SOH assessment is primarily focused on single cells, whereas their applicability to EV batteries at module or pack level is still limited and is not sufficiently investigated [18]. For instance, the battery is considered at EoL in EV applications if the remaining capacity dropped below 70% to 80% of its rated capacity. This does not mean all batteries in the pack reached their EoL due to series and parallel connections, which reflects only the capacity of the weakest battery within the pack [14]. Similarly, the resistance of the pack or module is affected by the heterogeneity between cells and interconnections [19]. As a result, understanding these issues is paramount to establish a robust SOH assessment scheme for EoL batteries that deals with modules and packs. In practice, two approaches are known to determine the SOH of a single cell: first, the impedance-based methods such as electrochemical-impedance spectroscopy (EIS) [20,21] and second the static capacity and its related techniques like incremental capacity analysis (ICA) [22,23]. Hitherto, there are few technical contributions regarding the extension of cell level diagnostics to module or pack level. The impedance-based method has been applied to monitor the SOH of a pack of four cylindrical cells connected in series [24,25]. The proposed approach utilised a single-frequency impedance diagnostic technique that was able to identify overcharge abuse of single cells without individual cell monitoring [24] and faults caused by low temperature degradation [25]. The same concept was adopted in [26] to monitor the SOH of parallel connected cells. Analysis of the EIS data and its corresponding SOH for the tested cells revealed that a change in imaginary impedance at the critical frequency can be correlated with the capacity fade. In [18], the impedance and ICA based techniques were experimentally evaluated in detecting abnormalities in series and parallel strings. The results revealed that both diagnostic methods were effective in detecting different extents of imbalance and ageing-related heterogeneity in series strings but struggle to discover similar abnormalities within parallel modules. Regardless of its short testing time, the performance of the EIS technique is sensitive and mainly affected by string size, state of charge (SOC), and temperature which restricts its utilisation in sorting retired EV modules due to the likely corrosion in module terminals, interconnections (inner module configuration), or any change in the cable leads that could potentially yield inaccurate grading outcomes. In addition, the high cost of electronics used to perform the EIS test including generating the signal, collecting, and processing data adds more challenges to its implementation in an industrial environment [24,27]. On the other hand, the capacity based methods are simple, straightforward, and requires less expensive equipment and cheap sensors to conduct the experiment in an industrial environment [28]. This includes, the direct discharge capacity determination, ICA, differential voltage analysis (DVA), and differential thermal voltammetry. Youlang et al. [14] studied the performance of retired EV modules for second life use by means of capacity and internal resistance characterisation. The residual capacity of the 24 modules was measured using several capacity test protocols and the hybrid pulse power characterisation (HPPC) test was utilised to estimate the internal resistance. The results demonstrated that high capacity is not always associated to small resistance and vice versa, given that each module has experienced different ageing process due to its location in the pack. Though a higher testing current without constant voltage (CV) stage was proposed to reduce duration of measurement, full charge/discharge cycle still required that implies long testing time. Ref [4] introduced an experimental cycle ageing of spent LIB modules from different Nissan Leaf EVs. To monitor the SOH of the modules, the discharge capacity and the internal resistance were measured periodically during the accelerated cycling tests. The evolution of these two health indicators was then used to identify the ageing knee of second life Leaf modules integrated in stationary application. Yet, the SOH assessment methods used in this study were time consuming as the fully charge and discharge cycles of the modules were needed to extract the related parameters. Due to their low computational power, the ICA and DVA methods are widely used to further analyse the capacity test results for more detailed battery information. Wang et al. [15] used an IC peak tracking approach to monitor the SOH of battery modules, which consist of battery cells with various ageing conditions. The findings suggest that the change in the IC curve peaks can be used as an indication of capacity fade in a battery module pack that has parallel-connected cells similar to a single cell case. Kalogiannis et al. [29] studied the implementation of ICA at a battery pack level using low charge current rates and concluded that the ICA method is applicable at pack level and can replicate accurately the actual SOH of the individual cells. The same notion was demonstrated in [30,31] where the characteristic peaks and valleys of the ICA on EV battery pack agree with the same on cell level that can be employed in SOH estimation.

Regardless of proving the utility of cell-based testing methods to module and pack level, the aforementioned studies were performed on packs and modules in usable conditions for primary applications with cycling data accessible to monitor the SOH evolution, which is not available in the case of sorting EoL packs and modules. This necessitates investigating the feasibility of these methods in the gateway testing process of EoL packs and modules with short testing time and limited data is available. To address this issue, SOH estimation using partial charge/discharge data was introduced in [32–36] at cell level and in [30] At pack level. Bian et al. [34] employed partial CC charge/discharge profiles to extract features of interest under the hood of ICA for the SOH estimation. Similarly, LIBs health prognosis method based

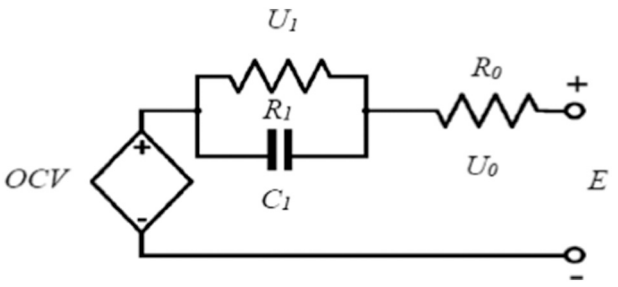

Fig. 1. The equivalent circuit model for LIB.

on partial IC curve is proposed in [33] and indicated that the health feature variables can be extracted from a particular voltage range that shows a remarkable change in the IC curve. In Ref. [32], the notion of regional capacity is introduced to establish a fast SOH estimation algorithm that focuses on the IC peak location hence requires only partial IC curves. Yang et al. [36] studied the relationship between the change in the interval capacity corresponding to a specific voltage region and battery ageing and then utilised this partial capacity with fractional impedance model for SOH estimation using the least-squares method. Although the partial charge discharge based methods can accurately estimate the SOH of LIBs, the data used in these studies are truncated from full charge/discharge process and no actual partial discharge data was utilised.

Based on the above considerations, the partial capacity during the discharge process is introduced in this study to determine the remaining capacity of retired battery modules from EVs where fully charge/discharge the batteries is not recommended to avoid wasting energy and to keep modules at desired SOC suitable for storage. The proposed solution comprised of a strategy that employs the ICA in detecting the informative region in the discharge curve that can be used to perform the partial discharge experiment to determine the full capacity utilising a reversed SOC estimation approach. The applicability of the proposed framework is investigated using a retired battery pack from Nissan Leaf EV. The discharge capacity measurements for 96 cell pairs encased in 48 modules are recorded and further analysed by means of ICA. The experimental results are shown in detail to validate the universality of using partial discharge in determining the remaining capacity without the need of performing full charge/discharge test.

2. Methodology

In this study, the measured terminal voltage and discharge current are deployed in the well-known coulomb counting method used in SOC estimation to estimate the full remaining capacity from only partial discharge data. For this purpose, the open circuit voltage (OCV)-SOC curve is firstly established, and a simple equivalent circuit model (ECM) is introduced to represent the internal and external behaviour of the cell pair during discharge process. Finally, the ICA is presented to analyse the discharge profile and to identify the targeted region for partial discharge experiment.

2.1. OCV-SOC table

For retired battery modules, some important information like OCV-SOC table is not available or needs to be updated due to ageing of the batteries. Therefore, the first step in sorting these modules is to obtain the experimental OCV-SOC curves either by low-current charge/discharge profile or by OCV sporadic testing [37–39]. Both methods require the full capacity to be measured beforehand and then apply a long resting period in the second method for the battery to reach the equilibrium status and coulomb counting in the low current test where the terminal voltage reflects the OCV at close-to-equilibrium status [38]. However, in this study, the OCV-SOC curve of each cell pair is unknown and is set to be the one obtained from one cell pair from the pack assuming that all modules have the same age in terms of the number of cycles applied during the vehicle use. In addition, Refs [37,40] confirmed that the OCV-SOC curves for LIBs from the same chemistry remain unchanged when normalised by "specific cell capacity" at different temperatures and ageing conditions.

2.2. Battery model

Fig. 1a demonstrates the general structure of the ECM, this model can be constructed from an ideal voltage source for OCV, ohmic resistance R_0, RC parallel branch(es). During high constant current discharge, the terminal voltage does not reflect the OCV and can be written as:

$$OCV = E + U_0 + U_1 \tag{1}$$

where U_0 is the voltage drop due to ohmic resistance, E is the terminal voltage, and U_1 is the RC branch voltage. Experimentally, the voltage

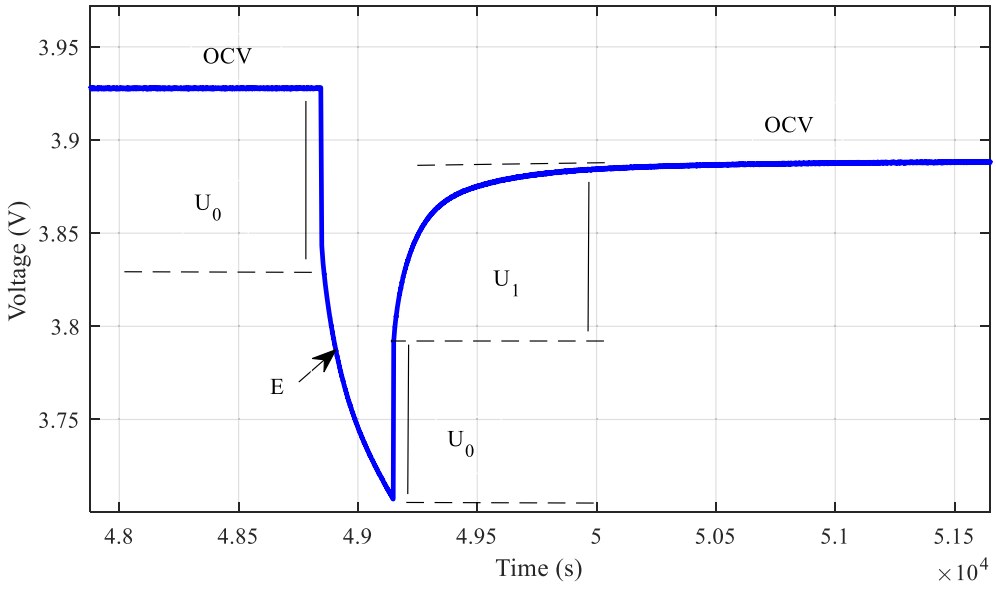

Fig. 2. A typical pulse discharge response for Leaf cell pair.

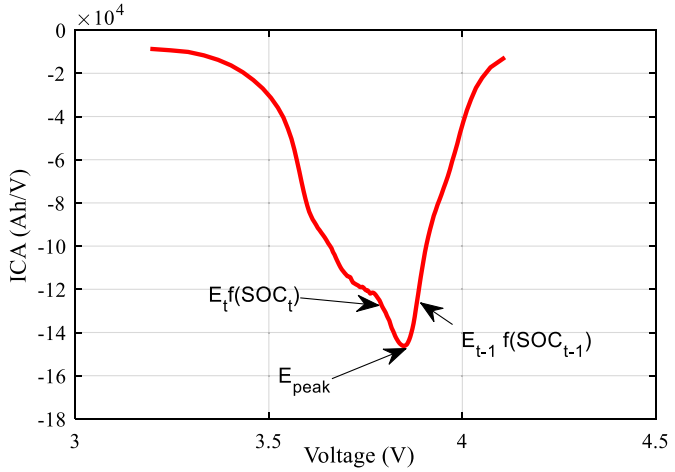

Fig. 3. An IC curve as a function of discharge voltage.

drop due to the ohmic resistance can be computed either from the falling edge of a voltage response pulse, and from the instantaneous voltage pull when current stops [41]. Due the parallel connection in battery modules, the authors confirmed that the R_0 is small (mΩ) and mostly dominated by the resistance of interconnection inside the module that is not affected by ageing [42]. Fig. 2 shows a typical partial discharge profile when a constant pulse discharge is applied for few minutes. In addition to the (U_0), the U_1 is calculated as the difference between the relaxation voltage (OCV) and the voltage drop due to R_0 (U_0). To simplify the calculations, the U_1 at a given SOC range is assumed to be constant for batteries that went under the same ageing conditions and can be computed from one cell pair for a predefined C rate and applied to the rest. As a result, the OCV can be estimated during constant current discharge from only terminal voltage and the SOC is inferred.

2.3. Full capacity estimation using partial discharge profile

Eq. (2) illustrates the estimated SOC under CC discharge process using the SOC-Q relation (coulomb counting):

$$SOC_t = SOC_{t-1} + \frac{\int_{t-1}^{t} Idt}{Q_{max}} \tag{2}$$

where SOC_t is the SOC at time t, SOC_{t-1} is the previously estimated SOC value or the initial SOC, I is the discharge current, and Q_{max} is the current maximum capacity of the cell pair. Apparently, if SOC_t and SOC_{t-1} are known from Eq. (1), the above formula can be manipulated to estimate unknown Q_{max} during the discharge process. However, this approach is strongly dependent on current and voltage measurement accuracy.

2.4. ICA

The open question here is how to determine the discharge pulse period and the appropriate SOC range to perform the experiment. To mitigate such challenges, the ICA is introduced here to extract some important features form the discharge profile. In this approach, the battery discharged capacity (Q) versus the terminal voltage (E) is differentiated to compute the IC curve as defined in Eq. (3) and transforming the plateaus in the E vs. Q charge/discharge curve to clearly identifiable peaks [15,43].

$$\frac{dQ}{dE} = \frac{Q_t - Q_{t-1}}{E_t - E_{t-1}} \tag{3}$$

where, Q_t, E_t are capacity and voltage values measured at a given time t respectively. Q_{t-1}, E_{t-1} are capacity and voltage values measured at a previous time $t - 1$. The IC peaks intensity, area, and position are quantitatively correlated to battery capacity and therefore it is used for SOH monitoring from single cells to multi-cell battery modules [15]. For these peaks to be detectable, using a low and constant charge/discharge current is proposed. Nevertheless, it was demonstrated in [30,43] that the peaks in an IC curve can also be identified when a higher current is used. In this paper, the same strategy introduced in [32] to locate the IC peak and identifying the region of interest is adopted to specify SOC_t and SOC_{t-1} used in the manipulated coulomb counting formula for full capacity estimation as illustrated in Fig. 3.

Table 1
BMS data.

Battery status	BMS data
Voltage (V)	371.54
Capacity (Ah)	50.49
State of charge (SOC) (%)	37.2
State of health (SOH) (%)	76.96
Hx (% of new battery conductance)	56.47
Voltage histogram (mV)	16
Odometer (mi)	40,420

3. Pack history and module description

First generation Nissan Leaf battery pack was acquired for this study after seven years of usage. Before the battery pack was removed from the EV, some underlying statistics provided by the battery management system (BMS) describing the status of the battery were recorded using a third party app called LeafSpy. The congregated information provides all the relevant data about the battery pack such as capacity, SOH, and driving distance as shown in Table 1. The SOH (i.e. the ratio of the current capacity to the initial capacity) of the battery stands at 76.96% and equates to 50.49 Ah. This index is anticipated to be the actual capacity of the weakest cell pair among the 96 cell pairs in the battery pack and is below the industry standard for EoL (SoH of 80% circa). As shown in Fig. 4(a), the original 24 kWh battery pack from the 2011 Nissan Leaf is made up of 48 modules configured in three module stacks in series. A horizontally placed 24 modules are arranged in the rear module stack, and the rest is equally divided between both sides of the front module stack in flat position.

Each module consists of four laminate pouch cells electrically configured as two cells in parallel pairs in series (2P2S). These pouch cells use lithium-manganese-oxide with nickel oxide (LiMn2O4 with LiNiO2) as a cathode material. Each module has three terminals red, white, and black (RWB). The red and black serve the positive and negative terminals of the module. The white terminal act as a positive or negative terminal relative to the two by two arrangement (see Fig. 4(b)). In this configuration, the cells' terminals are welded to copper bus bars to form the electrical connections for the module which means a direct access to individual cells is not feasible. As a result, and after pack disassembly, the 2P pairs either the RW or WB cell pairs are the smallest accessible unit in the module that will be tested in this work and will be referred to as cell pair. The Ampere hour rating and the nominal voltage for each cell pairs are 66 Ah and 3.75 V, respectively. The module canister has a dimension of (303 × 223 × 35 mm), and a weight of 3.8 kg.

4. Experimental setup and battery testing

The testing platform is displayed in Fig. 5, and it is mainly consisted of 48 retired modules from the Leaf pack, an HCP-1005 potentiostat from Bio-Logic, an environmental chamber, and a host computer with EC-Lab® software for experiment control and data storage.

To determine the discharge capacity, the Constant Current Constant Voltage (CCCV) protocol is chosen as a charging method followed by the CC procedure for discharging as shown in Fig. 6(a). During the charging stage, the cell pair is charged at 66 A (1C) to 4.2 V, then switched to a CV

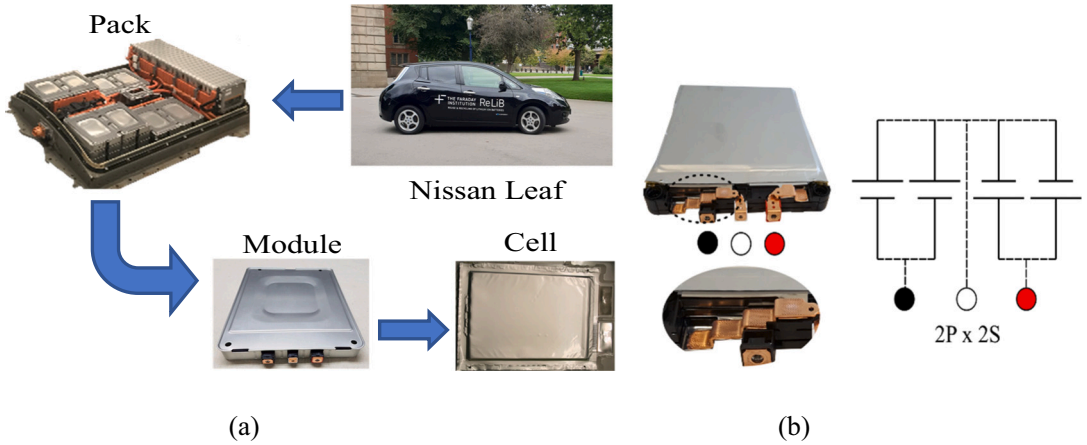

Fig. 4. Nissan Leaf battery pack. (a) Pack components. Electrical schematic of a Leaf module.

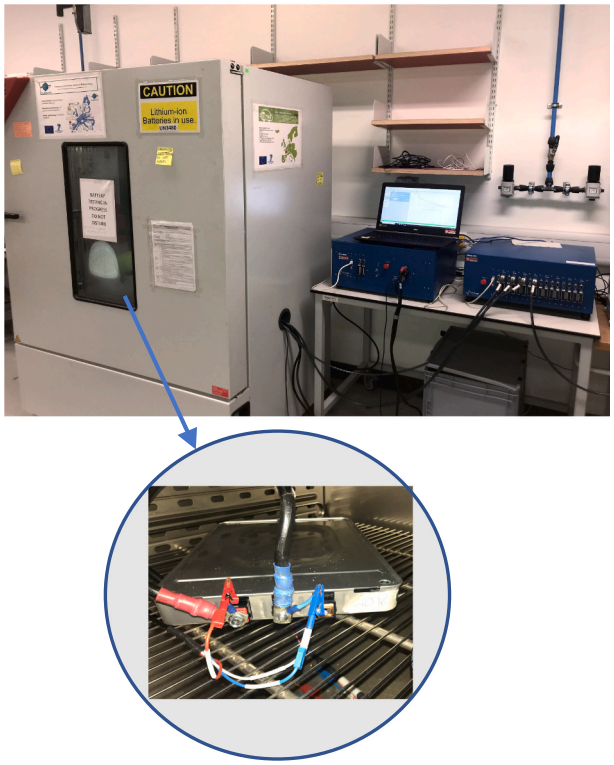

Fig. 5. Configuration of the module test bench.

phase until the current is less than C/20 (3.3 A). After 5 min of rest, the CC is applied to discharge the cell pair until the working voltage drops to 2.7 V.

To obtain the OCV-SOC table and other dynamic parameters, a randomly selected module from the pack was fully charged using CCCV protocol at C/20. After rest 2 h, the cell pair was discharged at the same C rate until the lower cutoff voltage is reached and the full capacity was recorded. Afterwards, the module was left to rest for 2 h and the same charge/discharge procedure was repeated to establish the OCV-SOC relationship as shown in Fig. 6(b). In this experiment, the terminal voltage measured at a low C-rate reflects the OCV at a close-to-equilibrium status. Following, the cell pair was recharged to 100% SOC upon the completion of the CCCV and left to rest for 1 h for the steady state, and then, the cell pair was discharged with constant current (CC) and ensure the decrease of SOC by 10%, to measure of the OCV after 1 h hence the U_p values over the entire SOC range. To emulate the real scenario in the battery recycling process, three modules from different module stacks were selected and partially charged to 4 V and left to rest for 1 h. Subsequently, the modules were discharged at 1C to obtain the partial discharge capacity measurements between different voltage ranges as shown in Fig. 6(c). It is worth noting that all the 96 cell pairs housed in the 48 modules were tested at 25 °C that is the temperature set for the thermal chamber, not the temperature of the cell pairs in the module.

5. Results and discussion

5.1. Discharge capacity

The battery discharge capacity represents the quantity of the electric charge that can be extracted from the battery by discharging from maximum operating voltage to minimum operating voltage under specified conditions [44]. It is determined by integrating of the discharge current over the discharge process from a fully charged battery and terminating at the minimum operating voltage that often refers to cut-off voltage [45]. The battery discharge capacity is typically measured in Ah and is used as convenient metric for defining the SOH of LIB [46–48]. The discharge capacity can also be quantified in Watt-hours (Wh) that measures the stored energy. Here, the SOH is defined as the ratio of the remaining capacity $Q_{current}$ in (Ah) to the nominal capacity of fresh cell pair $Q_{nominal}$ as depicted in Eq. (4):

$$SOH_Q = \frac{Q_{current}}{Q_{nominal}} \times 100 \tag{4}$$

In this paper, the discharge capacity for all 96 cell pairs from the retired pack was calculated by integrating the 1C (i.e., 66 A) discharge curves during the process described in the experimental setup. Fig. 7 shows that the rear module stack (RMS) has the lowest capacity measured just below 50 Ah which approximates the BMS data (SOH = 76.9%). The average capacity in the front left module stack (FLMS) is 54.37 Ah (SOH = 82%) that settles 2% beyond the limit. On the opposite side of the pack, the average capacity in the front right module stack (FRMS) is 51.51 Ah (SOH = 78%). Apart from four modules, all cell pairs were found to have comparable capacities. Although most cell pairs in the rear module stack have a capacity around of 50 Ah, three cell pairs whose capacity is higher than 54 Ah demonstrate that even modules within the same stack can experience different capacity fades. In general, 31% of the batteries were found to have >80% of the original capacity that endorses the trend towards refurbishing these batteries via reassembling them in packs to be reused in EV. This indicates that reusing the retired LIB from EVs is more beneficial at the module level than as a whole pack where the weakest module will dominate the overall performance. Indeed, in spite of the fact that the discharge

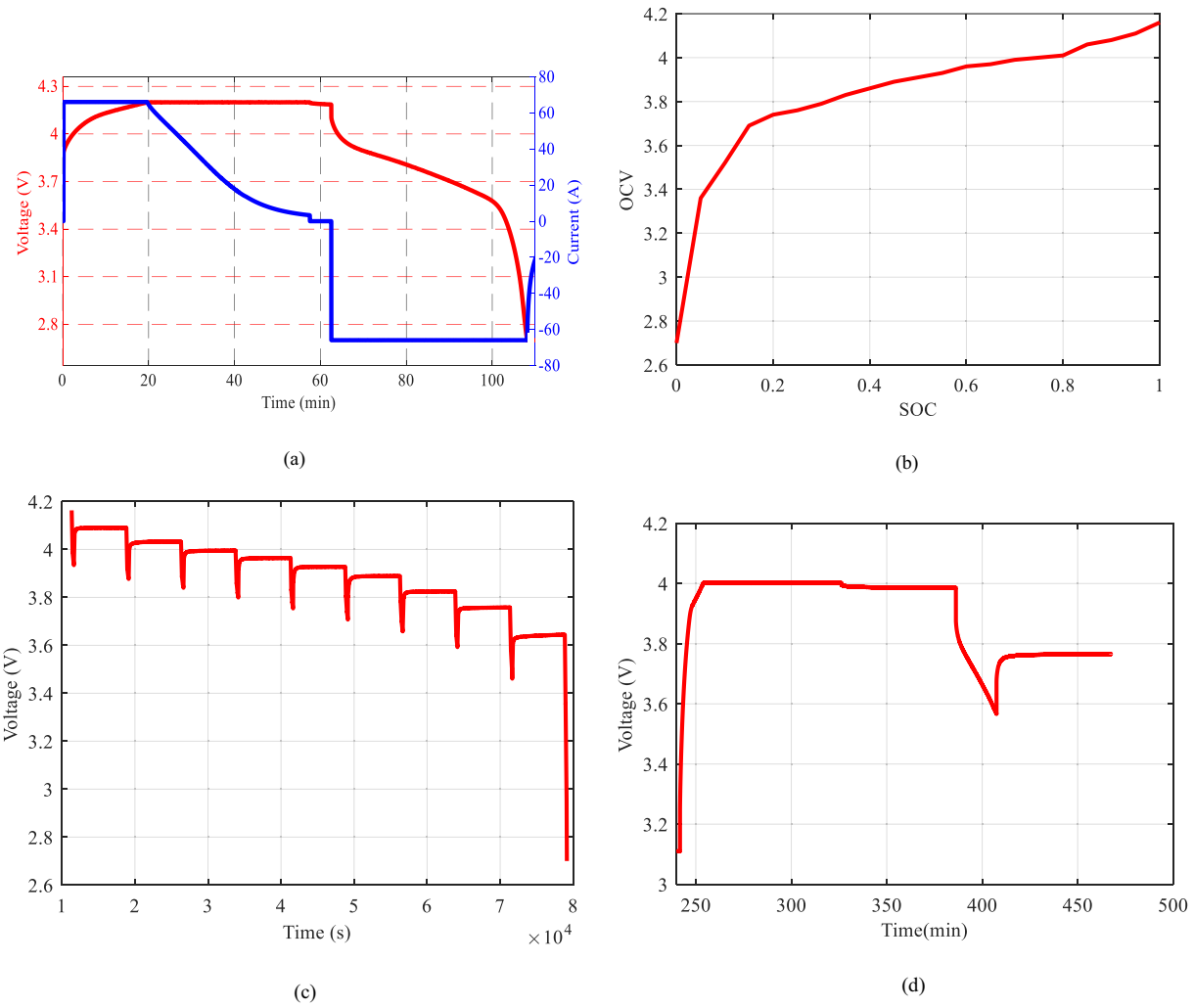

Fig. 6. Battery testing. (a) Discharge capacity test. (b) OCV-SOC curve. (c) Pulse discharge of 10% SOC step. (d) Partial charge/discharge test.

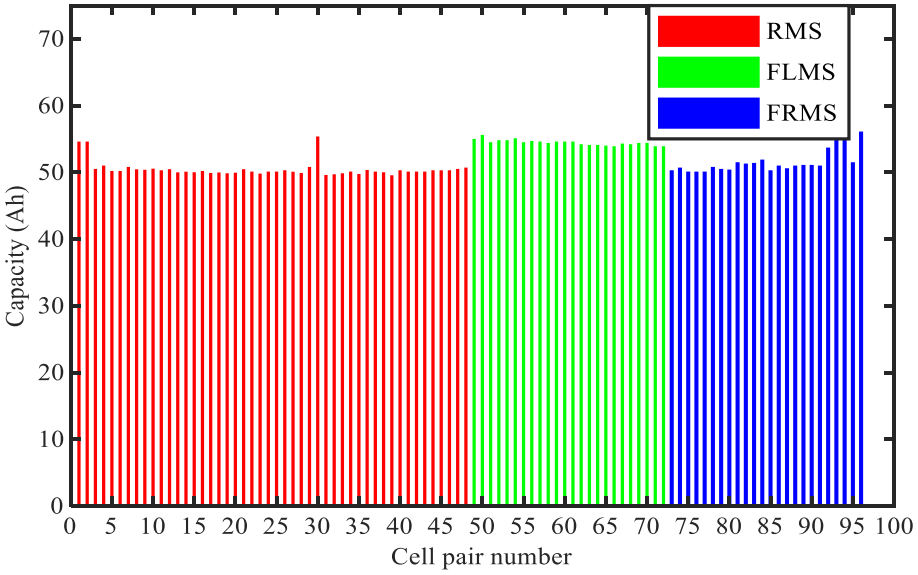

Fig. 7. Remaining capacities of all retired cell pairs from the Leaf pack.

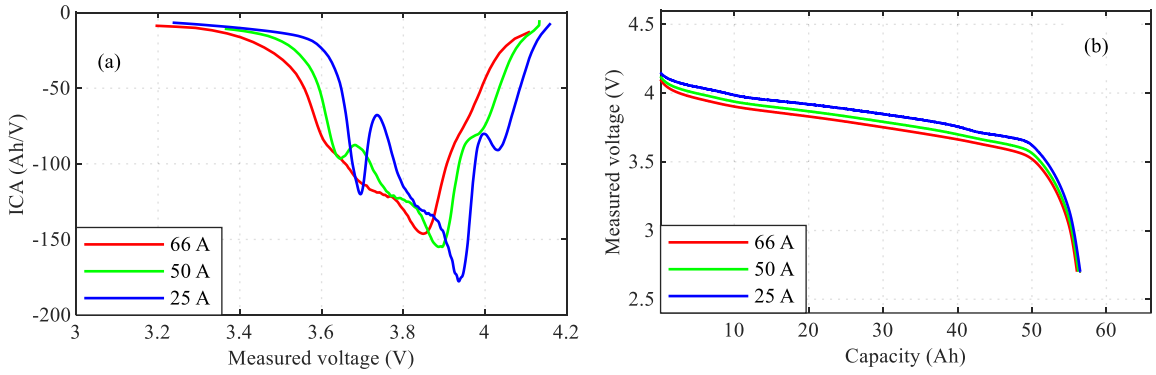

Fig. 8. ICA and voltage traces of 57 Ah cell pair under different discharging currents. (a) ICA, (b). Discharge capacity.

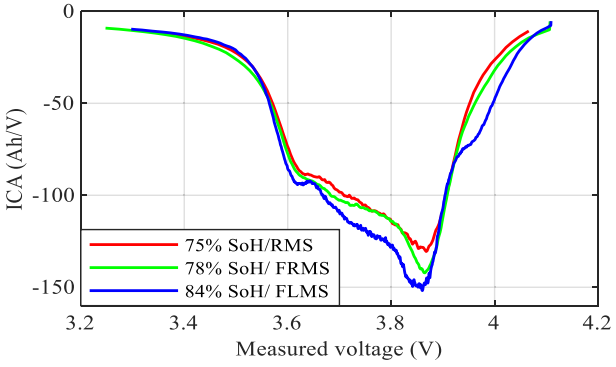

Fig. 9. Comparison of IC curves for cell pairs at different SOH.

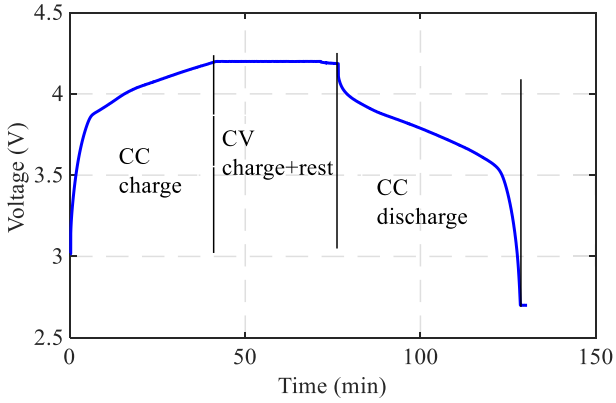

Fig. 10. Cell pair charge/discharge curve at 66 A.

capacity-based SOH estimation is precise, repeatable, and straight forward, this test is considered as a time-consuming process that requires the battery to be fully charged and discharged to carry out the current integration. This contradicts the aim of finding a rapid and accurate testing method to sort retired EV batteries based on their status for recycling, repurposing, or refurbishing. However, it is recommended to perform the full capacity test for at least one battery module from the pack to identify some characteristics related to the charge status of the LIB at the module level.

5.2. Incremental capacity analysis

Fig. 8. shows the change in the IC curve for 66A, 50A, and 25A discharging current applied on the strongest cell pair within the pack whose capacity is 57 Ah (SOH = 86%). As expected, the number of peaks was reduced from three identifiable peaks at 25A to only one peak at 66A, furthermore, the value of the remaining peak decreases as the discharging current rises resulting in a 25 Ah/V change in the IC peak amplitude within the same terminal voltage range (4–3.8 V) with a noticeable shift towards lower voltage. Besides, the discharge capacity was increased by less than 1 Ah. Therefore, the IC curve can be used as a health indicator even when a higher discharging current is used.

To elucidate the correlation between capacity and the peak value of the IC curve, the discharging data (66 A) for selected cell pairs with different capacities from the pack were processed. Fig. 9. shows the IC curves for selected cell pairs at the displayed SOH and their location in the pack. As one can observe, there is a clear reduction in the IC peak values as the capacity reduces that quantitatively reaches 20 Ah/V for 6 Ah difference in the measured capacity between the cell pair number 39 located in the RMS and cell pair 50 in the FLMS. This strengthens the validity of using IC peaks as a signature for battery capacity diminishing at the module level. According to electrochemistry hypotheses, there are three commonly reported battery degradation mechanisms identified as loss of lithium inventory, loss of active cathode material, and loss of active anode material. The IC analysis can help in identifying these modes; however, this involves a description of the cell chemistry, which is beyond the scope of this paper. Furthermore, this cannot be proved here as the LIBs are tested only once to assess their status, and no cycling is involved to monitor the change in the IC peaks. However, the ICA introduces a vital concept that refers to the most informative region (operating region) within the discharge curve where the IC peaks are located. This region was experimentally demonstrated for these cell pairs within the range of 4 V to 3.7 V when three different currents were used. In line with the capacity fade, the IC peaks height decrease and shift due to a loss of lithium inventory and/or active material [16,49,50]. To establish a time and cost-effective sorting procedure, only the discharge data at 66 A is studied in this paper that narrows the targeted region to the range 3.9 V to 3.8 V. This leads to introducing the partial discharge capacity (PDC) test in the following section as a quick and reliable SOH indicator in classifying retired EV batteries based on the stored energy in an industrial environment where the cost and testing time are paramount.

5.3. Partial discharge capacity (PDC)

Concretely, applying the full discharge capacity test in the industrial environment is impractical due to the time needed to perform the test. As depicted in Fig. 10, the charging time is almost about 70 min while the discharging time is 52 min. This data was extracted from the test applied on a fully discharged cell pair at 3.2 V to measure its capacity using the CCCV protocol. Fig. 7 also shows that only 11% of the charging time was taken to charge the battery from 3.2 V to 3.9 V using 35 Wh of energy, while 46% of the time was taken to charge the battery from 3.9 to 4.2 V which consumed around 150 Wh to fully charge the cell pair.

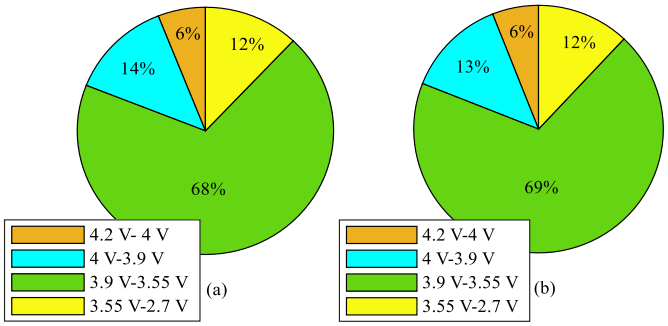

Fig. 11. Capacity distribution over full discharge curve. (a) Strongest cell pair, (b) Weakest cell pair.

Table 2
Full capacity estimation from truncated profile.

Module Number	E_{peak} (V)	PDC (Ah)	$\widetilde{Q}_{max}$ (Ah)	Q_{max} (Ah)
47RW	3.843	24.5	55	57
29BW	3.839	24	53	54
09RW	3.861	21.3	48	50

Similarly, the discharge time and energy recovered vary over the voltage range between 4.2 V and 2.7 V. Importantly, to ensure safety and prolong the cycle life many LIB manufacturers recommend avoiding fully charging/discharging their batteries and to keep them at approximately 40% SOC for safe storage. These facts inspired the proposed PDC technique using partial charge/discharge cycles that can greatly reduce the testing time and adhere to the safety measures for handling and storage of retired LIB modules.

5.3.1. *Truncated full discharge profile*

To evaluate the competence of PDC technique in predicting the full capacity, the discharge curve for the tested cell pairs was divided into three main regions: voltage between 4 V and 3.9 V, the voltage between 3.9 V and 3.55 V, and the third region between 3.55 V and 2.7 V. This division is based on the location of the IC peaks and to aid in selecting the adequate voltage region that can be used in full capacity evaluation. The PDC for each region named PDC1, PDC2, and PDC3 are recorded for all modules and outlined here for 3 cell pairs from the three different module stacks in the pack to represent the capacity range. From this data, almost 70% of the total energy for each cell pair is stored between 3.9 V and 3.55 V in all tested cell pairs, recording 40 Ah in cell pair 55 and 34.3 Ah in the weakest cell pair from the pack as shown in Fig. 11. Afterwards, using the IC curve to locate the peak voltage and region, the manipulated coulomb counting method is applied to estimate the full capacity $\widetilde{Q}_{\max}$ from the PDC2 profile with U_0 measured from the start of discharge and U_1 inferred from the reference module data to compute the OCV values. Table 2 illustrates the estimation results for the 0.2 V peak region with a maximum estimation error of 3% for the strongest cell pair. This peak region demonstrates the best estimation accuracy compared with 0.1 V and lower. Furthermore, the testing time to evaluate the capacity was reduced to less than 10 min instead of 52 min for full discharge. In addition to peak disappearance, the PDC1 and PDC3 show no clear correlation between partial and full capacity with differences hardly recognised between the strongest and weakest cell pairs.

The proposed approach was validated by measuring the partial discharge capacity for the remaining 93 cell pairs from the pack. The results obtained prove that the total discharge capacity can be accurately estimated through conducting the test for a single subregion with less than 3% estimation error.

5.3.2. *Actual partial discharge profile*

This section proves the feasibility of PDC in estimating the full capacity for partially charged batteries that is most likely to be the case in retired battery modules from EVs. Fig. 12a. shows the voltage response of partially charge cell pair to CC pulse discharge and the IC curve. Following the same procedure applied in the truncated profile, the IC curve was analysed, and the peak voltage was identified as displayed in Fig. 12b. Here, the initial SOC (SOC_{t-1}) is known from the OCV before the CC pulse is applied and only SOC_t is computed from Et according to Eq. (1). The results obtained in Table 3 demonstrate that the total discharge capacity can be estimated through conducting a CC discharge test on a partially charged battery with around a 2% estimation error higher than the truncated profile from the full test.

6. Conclusions

This paper has proposed a practical method based on using a partial

Table 3
Full capacity estimation from pulse discharge profile.

Module Number	E_{peak} (V)	PC (Ah)	$\widetilde{Q}_{max}$ (Ah)	Q_{max} (Ah)
47RW	3.685	23	54	57
29BW	3.725	19	51	54
09RW	3.735	16	48	50

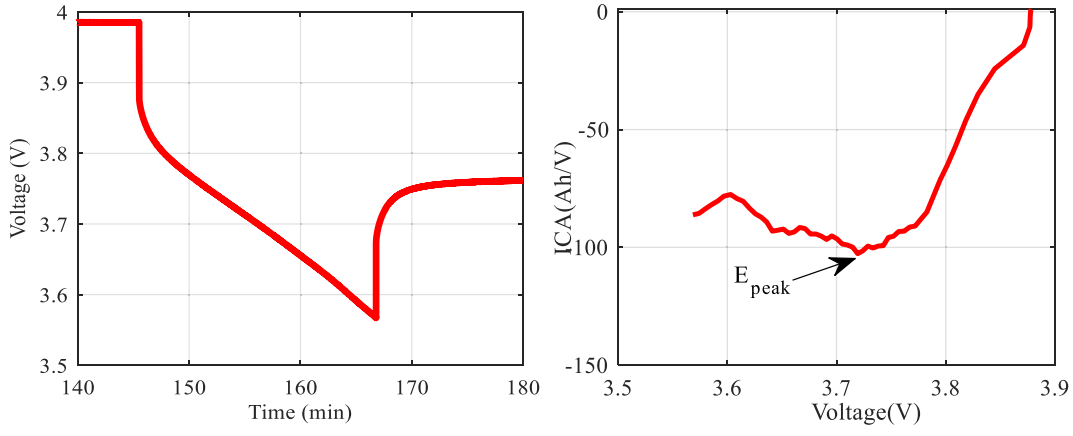

Fig. 12. Results of partial discharge. (a) Voltage response, (b) IC curve.

discharge profile to estimate the full capacity without the need to fully charge/discharge the retired module. Firstly, a simple ECM is introduced to represent the battery behaviour under the CC discharge current. Afterwards, the ICA was used to identify the informative region in the discharging capacity curve that includes the highest peak. Finally, manipulated coulomb counting approach is applied to compute the full capacity from the partial discharge profile. In this study, a retired 24 kWh battery pack from Nissan leaf was used to verify the accuracy of the proposed methods. The findings suggest that the ICA can be applied at the module level under high CC discharge to detect which segments of the discharge curve are most informative to implement the manipulated coulomb counting for full capacity estimation. As a result, the total capacity of retired LIB modules can be estimated with a maximum of 5% estimation error, if only a small portion of discharge data was considered in a short measurement time. Essentially, the testing time was significantly reduced to 10 min with a truncated profile and 20 min in the pulse discharge. However, the latter approach does not require fully charging the retired modules to be assessed which could save a tremendous amount of energy needed hence reducing the cost of the gateway testing in sorting a mass number of modules.

CRediT authorship contribution statement

All persons who meet authorship criteria are listed as authors, and all authors certify that they have participated sufficiently in the work to take public responsibility for the content, including participation in the concept, design, analysis, writing, or revision of the manuscript. Furthermore, each author certifies that this material or similar material has not been and will not be submitted to or published in any other publication before its appearance in the ***Journal of Energy Storage***.

Conception and design of study: M. Ahmeid, Musbahu Muhammad.

Acquisition of data: M. Ahmeid, Zoran Milojevic, Pierrot S. Attidekou.

Analysis and/or interpretation of data: M. Ahmeid, Zoran Milojevic, Musbahu Muhammad.

Drafting the manuscript: M. Ahmeid, Simon Lambert.

Revising the manuscript critically for important intellectual content: M. Ahmeid, Simon Lambert, Musbahu Muhammad.

Approval of the version of the manuscript to be published (the names of all authors must be listed): M. Ahmeid, Musbahu Muhammad, Zoran Milojevic, Pierrot S. Attidekou.

Declaration of competing interest

The authors declare that they have no known competing financial interests or personal relationships that could have appeared to influence the work reported in this paper.

Acknowledgements

This work was part of ReLiB project (https://relib.org.uk/) and was supported by the Faraday Institution [grant number FIRG005].

References

[1] X. Yuan, X. Li, Mapping the technology diffusion of battery electric vehicle based on patent analysis: a perspective of global innovation systems, Energy 222 (2021), 119897, https://doi.org/10.1016/j.energy.2021.119897, 2021/05/01/.

[2] D. Liu, J. Zhou, H. Liao, Y. Peng, X. Peng, A health indicator extraction and optimization framework for lithium-ion battery degradation modeling and prognostics, IEEE Trans. Syst. Man Cybern. Syst. Hum. 45 (6) (2015) 915–928, https://doi.org/10.1109/TSMC.2015.2389757.

[3] Y. Jiang, J. Jiang, C. Zhang, W. Zhang, Y. Gao, N. Li, State of health estimation of second-life LiFePO4 batteries for energy storage applications, J. Clean. Prod. 205 (2018) 754–762, https://doi.org/10.1016/j.jclepro.2018.09.149, 2018/12/20/.

[4] E. Braco, I. San Martín, A. Berrueta, P. Sanchis, A. Ursúa, Experimental assessment of cycling ageing of lithium-ion second-life batteries from electric vehicles, J. Energy Storage 32 (2020), 101695, https://doi.org/10.1016/j.est.2020.101695, 2020/12/01/.

[5] B.N.E. Finance, "Electric vehicle outlook 2017 [Online]. Available:, Bloomberg Finance LP, Tech. Rep, 2017 https://data.bloomberglp.com/bnef/sites/14/2017/07/BNEF_EVO_2017_ExecutiveSummary.pdf.

[6] G. Harper, et al., Recycling lithium-ion batteries from electric vehicles, Nature 575 (7781) (2019) 75–86, https://doi.org/10.1038/s41586-019-1682-5.

[7] A.S. Jacob, R. Banerjee, P.C. Ghosh, Trade-off between end of life of battery and reliability in a photovoltaic system, J. Energy Storage 30 (2020), 101565, https://doi.org/10.1016/j.est.2020.101565, 2020/08/01/.

[8] L. Ahmadi, S.B. Young, M. Fowler, R.A. Fraser, M.A. Achachlouei, A cascaded life cycle: reuse of electric vehicle lithium-ion battery packs in energy storage systems, Int. J. Life Cycle Assess. 22 (1) (2017) 111–124, https://doi.org/10.1007/s11367-015-0959-7.

[9] M. Cognet, J. Condomines, J. Cambedouzou, S. Madhavi, M. Carboni, D. Meyer, An original recycling method for li-ion batteries through large scale production of metal organic frameworks, J. Hazard. Mater. 385 (2020), 121603, https://doi.org/10.1016/j.jhazmat.2019.121603, 2020/03/05/.

[10] H. Vikström, S. Davidsson, M. Höök, Lithium availability and future production outlooks, Appl. Energy 110 (2013) 252–266, https://doi.org/10.1016/j.apenergy.2013.04.005, 2013/10/01/.

[11] X. Wang, G. Gaustad, C.W. Babbitt, K. Richa, Economies of scale for future lithium-ion battery recycling infrastructure, Resour. Conserv. Recycl. 83 (2014) 53–62, https://doi.org/10.1016/j.resconrec.2013.11.009, 2014/02/01/.

[12] C. Herrmann, A. Raatz, S. Andrew, J. Schmitt, Scenario-based development of disassembly systems for automotive lithium ion battery systems, Adv. Mater. Res. 907 (2014) 391–401, https://doi.org/10.4028/www.scientific.net/AMR.907.391.

[13] Y. Wu, L. Yang, X. Tian, Y. Li, T. Zuo, Temporal and spatial analysis for end-of-life power batteries from electric vehicles in China, Resour. Conserv. Recycl. 155 (2020), 104651, https://doi.org/10.1016/j.resconrec.2019.104651, 2020/04/01/.

[14] Y. Zhang, et al., Performance assessment of retired EV battery modules for echelon use, Energy 193 (2020), 116555, https://doi.org/10.1016/j.energy.2019.116555, 2020/02/15/.

[15] C. Weng, X. Feng, J. Sun, H. Peng, State-of-health monitoring of lithium-ion battery modules and packs via incremental capacity peak tracking, Appl. Energy 180 (2016) 360–368, https://doi.org/10.1016/j.apenergy.2016.07.126, 2016/10/15/.

[16] C. Pastor-Fernández, T.F. Yu, W.D. Widanage, J. Marco, Critical review of non-invasive diagnosis techniques for quantification of degradation modes in lithium-ion batteries, Renew. Sust. Energ. Rev. 109 (2019) 138–159, https://doi.org/10.1016/j.rser.2019.03.060, 2019/07/01/.

[17] M. Dubarry, C. Pastor-Fernández, G. Baure, T.F. Yu, W.D. Widanage, J. Marco, Battery energy storage system modeling: investigation of intrinsic cell-to-cell variations, J. Energy Storage 23 (2019) 19–28, https://doi.org/10.1016/j.est.2019.02.016, 2019/06/01/.

[18] T.R. Tanim, E.J. Dufek, L.K. Walker, C.D. Ho, C.E. Hendricks, J.P. Christophersen, Advanced diagnostics to evaluate heterogeneity in lithium-ion battery modules, eTransportation 3 (2020) 100045, https://doi.org/10.1016/j.etran.2020.100045, 2020/02/01/.

[19] L. Xie, et al., A facile approach to high precision detection of cell-to-cell variation for li-ion batteries, Sci. Rep. 10 (1) (2020) 7182, https://doi.org/10.1038/s41598-020-64174-2, 2020/04/28.

[20] R.A. Nazer, V. Cattin, P. Granjon, M. Montaru, M. Ranieri, Broadband identification of battery electrical impedance for HEVs, IEEE Trans. Veh. Technol. 62 (7) (2013) 2896–2905, https://doi.org/10.1109/TVT.2013.2254140.

[21] D. Andre, M. Meiler, K. Steiner, C. Wimmer, T. Soczka-Guth, D.U. Sauer, Characterization of high-power lithium-ion batteries by electrochemical impedance spectroscopy. I. Experimental investigation, J. Power Sources 196 (12) (2011) 5334–5341, https://doi.org/10.1016/j.jpowsour.2010.12.102, 2011/06/15/.

[22] X. Li, J. Jiang, L.Y. Wang, D. Chen, Y. Zhang, C. Zhang, A capacity model based on charging process for state of health estimation of lithium ion batteries, Appl. Energy 177 (2016) 537–543, https://doi.org/10.1016/j.apenergy.2016.05.109, 2016/09/01/.

[23] C. Weng, Y. Cui, J. Sun, H. Peng, On-board state of health monitoring of lithium-ion batteries using incremental capacity analysis with support vector regression, J. Power Sources 235 (2013) 36–44, https://doi.org/10.1016/j.jpowsour.2013.02.012, 2013/08/01/.

[24] C.T. Love, M.B.V. Virji, R.E. Rocheleau, K.E. Swider-Lyons, State-of-health monitoring of 18650 4S packs with a single-point impedance diagnostic, J. Power Sources 266 (2014) 512–519, https://doi.org/10.1016/j.jpowsour.2014.05.033, 2014/11/15/.

[25] C.T. Love, et al., Lithium-ion cell fault detection by single-point impedance diagnostic and degradation mechanism validation for series-wired batteries cycled at 0 C, Energies 11 (4) (2018) 834, https://doi.org/10.3390/en11040834.

[26] B. Huhman, Single-frequency battery state-of-health diagnostic for LiFePO4 cells in 4P1S array, ECS Meet. Abstr. (2017), https://doi.org/10.1149/MA2017-02/4/398.

[27] R.Al Nazer, V. Cattin, P. Granjon, M. Montaru, M. Ranieri, Broadband identification of battery electrical impedance for HEVs, IEEE Trans. Veh. Technol. 62 (7) (2013) 2896–2905, https://doi.org/10.1109/TVT.2013.2254140. Art no. 6516985.

[28] Y. Merla, B. Wu, V. Yufit, N.P. Brandon, R.F. Martinez-Botas, G.J. Offer, Extending battery life: a low-cost practical diagnostic technique for lithium-ion batteries, J. Power Sources 331 (2016) 224–231, https://doi.org/10.1016/j.jpowsour.2016.09.008, 2016/11/01/.

[29] T. Kalogiannis, D.I. Stroe, J. Nyborg, K. Nørregaard, A.E. Christensen, E. Schaltz, Incremental capacity analysis of a lithium-ion battery pack for different charging rates, ECS Trans. 77 (11) (2017) 403–412, https://doi.org/10.1149/07711.0403ecst, 2017/07/07.

[30] E. Schaltz, D.I. Stroe, K. Nørregaard, L.S. Ingvardsen, A. Christensen, Incremental capacity analysis applied on electric vehicles for battery state-of-health estimation, IEEE Trans. Ind. Appl. 57 (2) (2021) 1810–1817, https://doi.org/10.1109/TIA.2021.3052454.
[31] A. Thingvad, L. Calearo, P.B. Andersen, M. Marinelli, Empirical capacity measurements of electric vehicles subject to battery degradation from V2G services, IEEE Trans. Veh. Technol. 70 (8) (2021) 7547–7557, https://doi.org/10.1109/TVT.2021.3093161.
[32] X. Tang, et al., A fast estimation algorithm for lithium-ion battery state of health, J. Power Sources 396 (2018) 453–458, https://doi.org/10.1016/j.jpowsour.2018.06.036, 2018/08/31/.
[33] X. Li, Z. Wang, J. Yan, Prognostic health condition for lithium battery using the partial incremental capacity and gaussian process regression, J. Power Sources 421 (2019) 56–67, https://doi.org/10.1016/j.jpowsour.2019.03.008, 2019/05/01/.
[34] X. Bian, Z. Wei, J. He, F. Yan, L. Liu, A novel model-based voltage construction method for robust state-of-health estimation of lithium-ion batteries, IEEE Trans. Ind. Electron. 68 (12) (2021) 12173–12184, https://doi.org/10.1109/TIE.2020.3044779.
[35] D. Liu, Y. Song, L. Li, H. Liao, Y. Peng, On-line life cycle health assessment for lithium-ion battery in electric vehicles, J. Clean. Prod. 199 (2018) 1050–1065, https://doi.org/10.1016/j.jclepro.2018.06.182, 2018/10/20/.
[36] Q. Yang, J. Xu, X. Li, D. Xu, B. Cao, State-of-health estimation of lithium-ion battery based on fractional impedance model and interval capacity, Int. J. Electr. Power Energy Syst. 119 (2020), 105883, https://doi.org/10.1016/j.ijepes.2020.105883, 2020/07/01/.
[37] B. Pattipati, B. Balasingam, G.V. Avvari, K.R. Pattipati, Y. Bar-Shalom, Open circuit voltage characterization of lithium-ion batteries, J. Power Sources 269 (2014) 317–333, https://doi.org/10.1016/j.jpowsour.2014.06.152, 2014/12/10/.
[38] M. Petzl, M.A. Danzer, Advancements in OCV measurement and analysis for lithium-ion batteries, IEEE Trans. Energy Convers. 28 (3) (2013) 675–681, https://doi.org/10.1109/TEC.2013.2259490.
[39] B. Sun, et al., Practical state of health estimation of power batteries based on Delphi method and grey relational grade analysis, J. Power Sources 282 (2015) 146–157, https://doi.org/10.1016/j.jpowsour.2015.01.106, 2015/05/15/.
[40] M. Dubarry, N. Vuillaume, B.Y. Liaw, From single cell model to battery pack simulation for li-ion batteries, J. Power Sources 186 (2) (2009) 500–507.
[41] A. Barai, K. Uddin, W.D. Widanage, A. McGordon, P. Jennings, A study of the influence of measurement timescale on internal resistance characterisation methodologies for lithium-ion cells, Sci. Rep. 8 (1) (2018) 21, https://doi.org/10.1038/s41598-017-18424-5, 2018/01/08.
[42] M. Ahmeid, M. Muhammad, Z. Milojevic, S. Lambert, P. Attidekou, The energy loss due to interconnections in paralleled cell configurations of lithium-ion batteries in electric vehicles, in: 2019 IEEE 4th International Future Energy Electronics Conference (IFEEC), 25-28 Nov. 2019, 2019, pp. 1–4, https://doi.org/10.1109/IFEEC47410.2019.9014956.
[43] C. Weng, J. Sun, H. Peng, A unified open-circuit-voltage model of lithium-ion batteries for state-of-charge estimation and state-of-health monitoring, J. Power Sources 258 (2014) 228–237, https://doi.org/10.1016/j.jpowsour.2014.02.026, 2014/07/15/.
[44] A. Kirchev, Battery management and battery diagnostics, in: Electrochemical Energy Storage for Renewable Sources and Grid Balancing, Elsevier, 2015, pp. 411–435.
[45] C. Nebl, F. Steger, H.-G. Schweiger, Discharge capacity o f energy storages as a function of the discharge current–expanding peukert's equation, Int. J. Electrochem. Sci. 12 (6) (2017) 4940–4957, https://doi.org/10.20964/2017.06.51.
[46] D. Stroe, E. Schaltz, Lithium-ion battery state-of-health estimation using the incremental capacity analysis technique, IEEE Trans. Ind. Appl. 56 (1) (2020) 678–685, https://doi.org/10.1109/TIA.2019.2955396.
[47] A. Basia, Z. Simeu-Abazi, E. Gascard, P. Zwolinski, Review on state of health estimation methodologies for lithium-ion batteries in the context of circular economy, CIRP J. Manuf. Sci. Technol. 32 (2021) 517–528, https://doi.org/10.1016/j.cirpj.2021.02.004, 2021/01/01/.
[48] Y. Guo, K. Huang, X. Hu, A state-of-health estimation method of lithium-ion batteries based on multi-feature extracted from constant current charging curve, J. Energy Storage 36 (2021), 102372, https://doi.org/10.1016/j.est.2021.102372, 2021/04/01/.
[49] B. Jiang, H. Dai, X. Wei, Incremental capacity analysis based adaptive capacity estimation for lithium-ion battery considering charging condition, Appl. Energy 269 (2020), 115074, https://doi.org/10.1016/j.apenergy.2020.115074, 2020/07/01/.
[50] A. Fly, R. Chen, Rate dependency of incremental capacity analysis (dQ/dV) as a diagnostic tool for lithium-ion batteries, J. Energy Storage 29 (2020), 101329, https://doi.org/10.1016/j.est.2020.101329, 2020/06/01/.